Numerical Analysis of a De-Laval Nozzle using CFD software

Noe Lepez Da Silva Duarte
Georgia Institute of Technology, Atlanta, GA, 30309

AE 4803 - Spring 2022

Dr. Joseph Saleh
Dr. Stephen Ruffin

Abstract

A De-Laval nozzle is made up of a converging and a diverging section used to accelerate fluid to supersonic velocities due to the change in cross-sectional area. However, this is only possible when the nozzle's exit pressure is low enough to allow the fluid to expand. Normal shocks occur in the diverging section if this condition is not met, slowing the fluid down to subsonic velocity. As such, this survey investigates the performance of a De-Laval nozzle at sea level with a range of back pressures, using the ANSYS package and Fluent, a computational fluid dynamics software which uses numerical analysis methods. The flow was assumed to be inviscid and followed expected velocity-static pressure relationships; when velocity increases, static pressure decreases. Normal shocks appeared at a pressure ratio of 0.8 and got closer to the outlet as the pressure ratio was decreased. Finally, the nozzle became fully supersonic once the backpressure reached half of the inlet pressure, indicating that the optimal pressure ratio for a fully supersonic nozzle occurs between 0.6 and 0.5 pressure ratio.

I. Introduction

Invented by Gustaf de Laval, a De-Laval nozzle is a converging-diverging type of nozzle with many applications, ranging from increasing supersonic aircraft exhaust velocity to rocket engines nozzles. Often used to accelerate subsonic fluid to supersonic speeds to increase the thrust of air-breathing engines and rockets, De-Laval nozzles can be designed to control properties of fluid-like pressure, density, temperature, and velocity [1]. In this paper, a De-Laval nozzle is designed and analyzed using the Computation Fluid Dynamics (CFD) software ANSYS FLUENT. It is tested at sea level conditions and with different pressure ratios to investigate the nozzle's performance and compare the accuracy of modeled data with expected results.

As stated prior, De-Laval nozzles are primarily used to accelerate flows to supersonic velocities. To do so, they are split into two sections, a converging section, and a diverging nozzle. The converging nozzle's cross-section is reduced down to the throat (the point with the smallest cross-section where the converging and diverging sections meet), where the fluid achieves maximum velocity and minimum static pressure. With appropriate conditions, the fluid can reach sonic speeds at this location (Mach number = 1), which would further accelerate in the nozzle's diverging section. It is assumed that the fluid is isentropic, inviscid, and compressible. Therefore, as the mass flow rate stays constant, the speed of subsonic fluid increases with decreasing cross-sectional area due to the decrease in static pressure as given by Bernoulli's law. Choked flow occurs when the flow's local velocity becomes sonic. However, having a choked flow isn't equal to having supersonic flow at the nozzle's end. Indeed, the supersonic fluid may decelerate in the diverging section due to high back pressure (pressure at the nozzle's exit), causing chocks. As such, the state of the exiting nozzle flow depends on the pressure ratio, Pr,

$$\mathrm{Pr} = \frac{Ambient\ pressure\ at\ Outlet}{Inlet\ pressure} = \frac{Pb}{Po} \tag{1}$$

Figure 1 shows numerous possible pressure variations for given back pressures. Five separate situations can be defined for a De-Laval nozzle:

If $P_0=P_b$, there is no pressure difference throughout the nozzle and therefore no flow, shown by the horizontal dashed line in Fig. 1.

If $P_0>P_b>P_c$, where P_c is the critical pressure at which the flow becomes sonic, the flow gains speed in the converging nozzles, reaches a maximum at the throat and loses speed in the nozzle's

diverging section. On the contrary, the pressure will decrease until the throat is reached and increase to reach the back pressure in the diffuser, as shown by cases (a) and (b).

If $P_b=P_c$, the flow reaches sonic velocity at the throat.

If $P_c>P_b>P_e$, where P_e is the pressure at the nozzle's exit, the fluid reaches sonic velocity at the throat and continues accelerating in the diverging section. However, as the back pressure is higher than the exit pressure, the flow stops accelerating creating normal shocks in the diffuser. This is caused by the gas suddenly expanding to match the ambient pressure at the outlet, causing the flow to become subsonic again. In the special case that $P_b=P_e$, normal shocks are created at the exit. Due to the presence of a normal shock, the flow cannot be considered to be isentropic in this case. These are shown as cases (c) and (d) in Fig. 1.

Finally, if $P_e>P_b>0$, the flow becomes sonic at the throat and continues to accelerate until it leaves the nozzle at supersonic speeds as seen in case (f) in Fig. 1. [2]

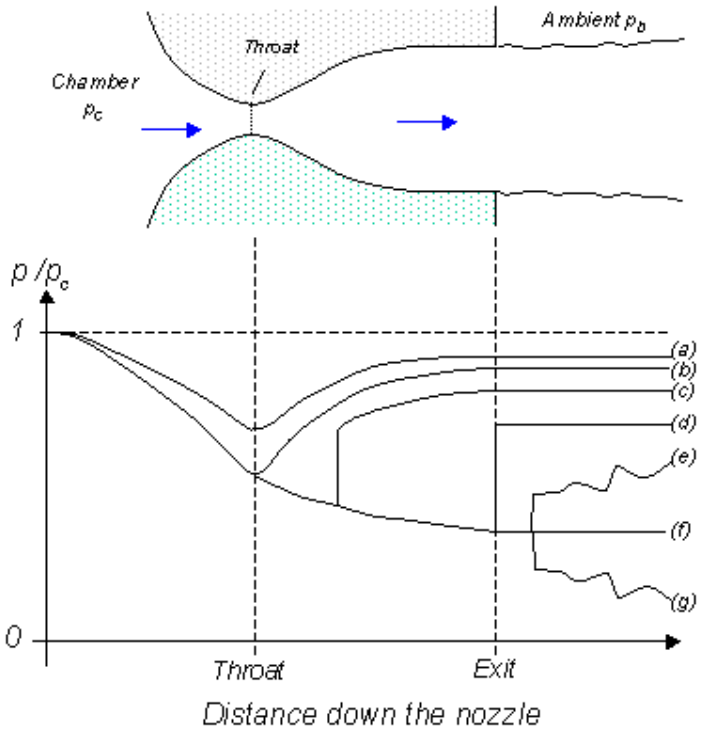

Figure 1. Variation in static pressure over stagnation pressure for different back pressures [3]

The following equations show how pressure, density, ρ, and temperature, T, can be related to their stagnation counterparts. In addition, eq. 5 shows how Mach number relates to the nozzle's cross-sectional area, A, and eqs. 6 and 7 shows how to calculate sound speed, a, and how it relates to Mach number, M and velocity, V.

$$\frac{P}{P_t} = \left[\frac{1}{1+\frac{\gamma-1}{2}M^2}\right]^{\frac{\gamma}{\gamma-1}} \tag{2}$$

$$\frac{\rho}{\rho_t} = \left[\frac{1}{1+\frac{\gamma-1}{2}M^2}\right]^{\frac{1}{\gamma-1}} \tag{3}$$

$$\frac{T}{T_t} = \frac{1}{1+\frac{\gamma-1}{2}M^2} \tag{4}$$

$$\frac{A}{A^*} = \frac{1}{M}\left[\frac{1+\frac{\gamma-1}{2}}{1+\frac{\gamma-1}{2}M^2}\right]^{\frac{-(\gamma+1)}{2(\gamma-1)}} \tag{5}$$

$$a = \sqrt{\gamma RT} \tag{6}$$

$$V = M\,a \tag{7}$$

II. Problem formulation

Computer simulation of the nozzle was achieved using CFD, using the ANSYS Workbench software. This software allows users to easily model, mesh, setup, solve and plot any CFD case by using ANSYS applications such as the design modeler, meshing and Fluent.

Modelling

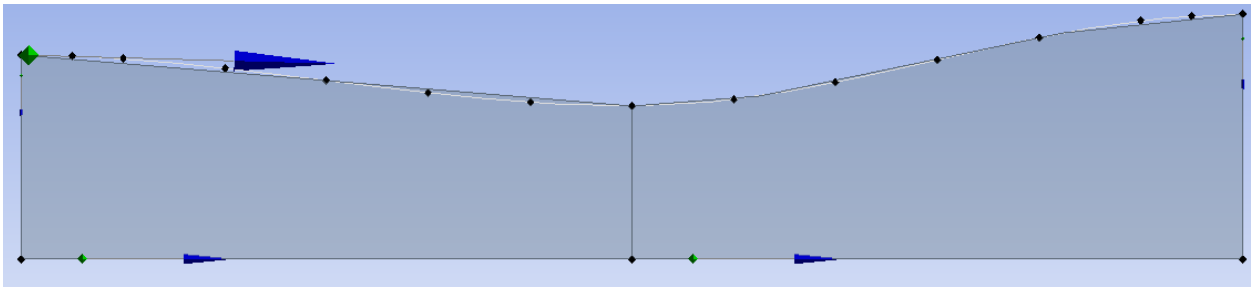

Figure 2. Design of De-Laval Nozzle

A De-Laval nozzle was designed using ANSYS Design modeler using the help of tutorials [4]. Numerous designs were made and tested for this project. However, any unusual throat made Fluent have issues finding steady-state solutions. As such, the nozzle's walls were made using a set of points and lines and modified to have the convergence and divergence angles given in Table I. Once the sketch was completed, a surface was made from the sketch, seen in gray on Fig. 2. Additional vertical lines were added in locations where the wall's gradient changed to split the faces for easy meshing. Separate faces were created by adding "Face split" and selecting the vertical lines. The dimensions are tabulated in Table I.

Table I. Dimensions of De-Laval Nozzle

Parameter	Dimension
Total length (mm)	84
Inlet Diameter (mm)	28
Outlet Diameter (mm)	34
Throat Diameter (mm)	21
Convergence angle (deg)	25
Divergence angle (deg)	20

Meshing

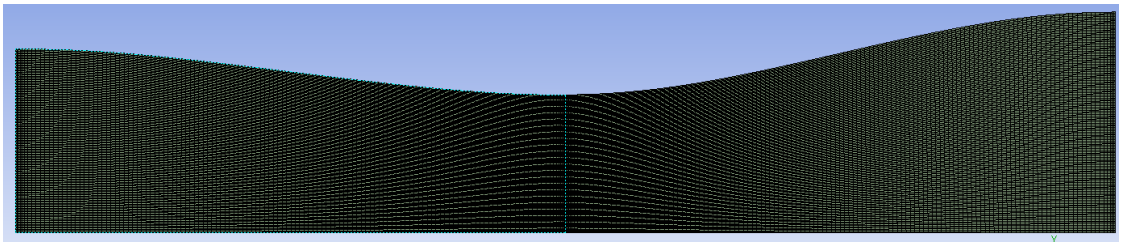

Figure 3. De-Laval nozzle mesh

Meshing was completed in the ANSYS meshing software. As the surface had been split into two separate surfaces, numerous meshes were created for each surface. Indeed, 150 divisions were created along the vertical edges, and 175 on each first horizontal surface. The surface was split in the throat's center to create a uniform mesh with close to rectangular cells. Finally, a face meshing using quadrilaterals was added to refine the mesh. This resulted in a high-quality mesh with minimal warping, 39900 nodes and 39485 elements. The mesh is shown in Fig. 3; however, it is hard to see due to the high density of elements. Figure 4 shows the mesh at the throat.

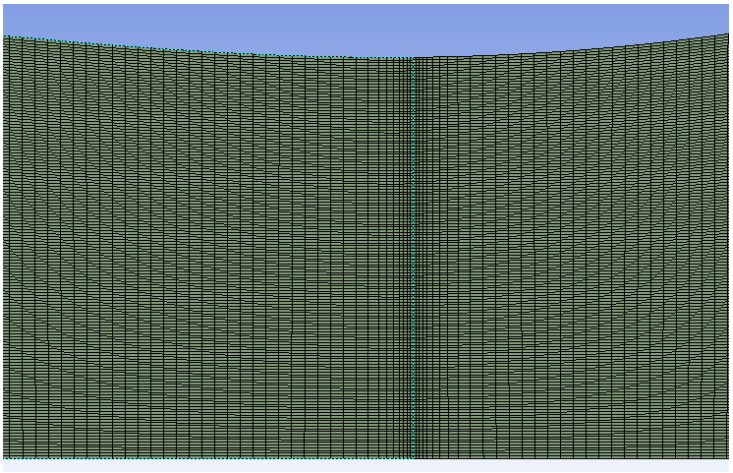

Figure 4. Mesh at the throat

Pre-processing

As the model was simulated using the ANSYS Fluent software, all pre-processing was done in Fluent to make the software use appropriate models, boundary conditions and use specific settings shown in Table II.

Table II. Pre-processing details.

General	Solver type: Density-based 2D Space: Planar Time: Steady
Spatial Discretization	Gradient: Least Squares Cell Based Flow: First Order Upwind
Materials	Energy model: On Density: Ideal Gas Thermal Conductivity: 0.02619 W/mK C_p: 1006.43 J/(kg K) Molecular weight: 28.966 kg/kmol

Table III. shows the boundary conditions set in each case.

Table III. Boundary conditions.

Boundary conditions	Inlet pressure: 101325 Pa Inlet Temperature: 288.15 K Outlet Temperature: 288.15 K

Table IV shows pressure ratios and resulting back pressures for each test case.

Table IV. Pressure ratio and back pressure for each test case.

Case	**Pressure ratio**	**Back Pressure (P_b)**
I	0.95	96258.75
II	0.80	81060.0
III	0.70	70927.5
IV	0.60	60795.0
VI	0.50	50662.5
VII	0.40	40530.0

Upwind Scheme

All experiments in this paper were completed using ANSYS's first order upwind scheme. It is the simplest and most stable discretization scheme; however, it is it is more dissipative and cannot model numerous viscous effects. As such, it will converge more easily while being less accurate than a higher order scheme (as was learned in Module V). This scheme works by taking upstream values of the flow, at cell boundaries, to evaluate the values at the cell's center [5]. As such, the first order upwind scheme only considers one point behind, while the second order scheme considers two. Indeed, this scheme uses finite difference approximations to solve equations similar to the advection equation (in one-dimension here),

$$\frac{\delta u}{\delta t} + a\frac{\delta u}{\delta x} = 0 \tag{8}$$

And can be solved as

$$u_i^{n+1} = u_i^n - \Delta t[a^+ u_x^- + a^- u_x^+] \tag{9}$$

$$u_x^- = \frac{u_i^n - u_{i-1}^n}{\Delta x}, u_x^+ = \frac{u_{i+1}^n - u_i^n}{\Delta x} \tag{10}$$

Where i represents the cell number, n the iteration step, a is a constant and u is the variable to be solved (velocity in this case) [6]. The equations above are a simplified version of the commercial code used in FLUENT, nevertheless, these provide a good basis to understand how the scheme functions. In addition, the software uses LU decomposition to solve x, y, z velocities, pressure, p, and temperature, T [7],

$$\frac{\delta \mathrm{Q}}{\delta t} + \frac{\delta \mathrm{E}}{\delta \mathrm{x}} + \frac{\delta \mathrm{F}}{\delta \mathrm{y}} + \frac{\delta \mathrm{G}}{\delta \mathrm{z}} = L(Q_v) \tag{11}$$

$$Q(x,t) = \begin{pmatrix} \rho \\ \rho u \\ \rho v \\ \rho w \\ \rho e_t \end{pmatrix}, Q_v(x,t) = \begin{pmatrix} \mathrm{p} \\ u \\ v \\ w \\ \mathrm{T} \end{pmatrix}, E(x,t) = \begin{pmatrix} \rho \mathrm{u} \\ \rho u \mathrm{u} + \mathrm{p} \\ \rho v \mathrm{u} \\ \rho w \mathrm{u} \\ (\rho e_t + p)u \end{pmatrix}, \text{etc.} \tag{12}$$

While using a second order upwind scheme would have been more accurate, the hardware had trouble running simulations while testing (see Appendix B).

Throughout the trials in part III, cases were first run for 2000 iterations with a step size of 1. Should the residuals appear to be decreasing, the step size would slowly be increased to 3 for 1000

iterations, and eventually 5 to allow the simulation to finish faster. However, the mesh had to be updated numerous times to ensure the mesh was fine enough and continuous to allow for satisfactory results. Indeed, the simulation often had issues, and diverged due to an unsatisfactory mesh, or unconventional nozzle geometry.

III. Results and discussion

Each case only shows the nozzle's top half; however, these were calculated assuming a symmetric top and bottom. Residuals for each case can be found in Appendix A.

Case I.

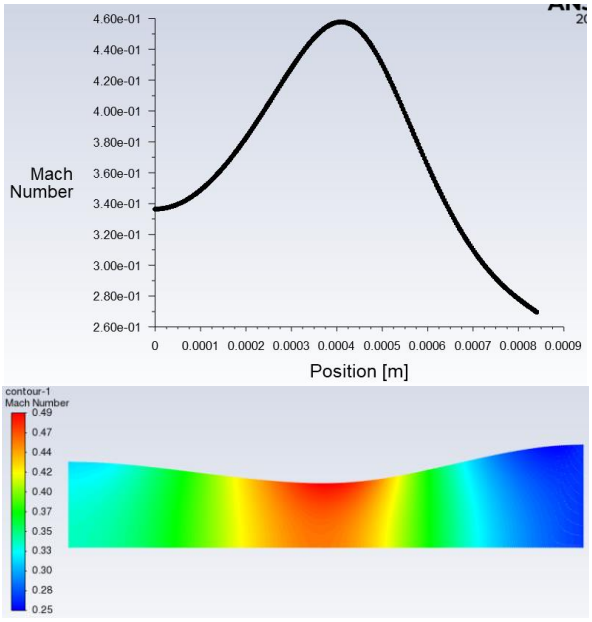

Figure 5. Mach number contour for Pr = 0.95

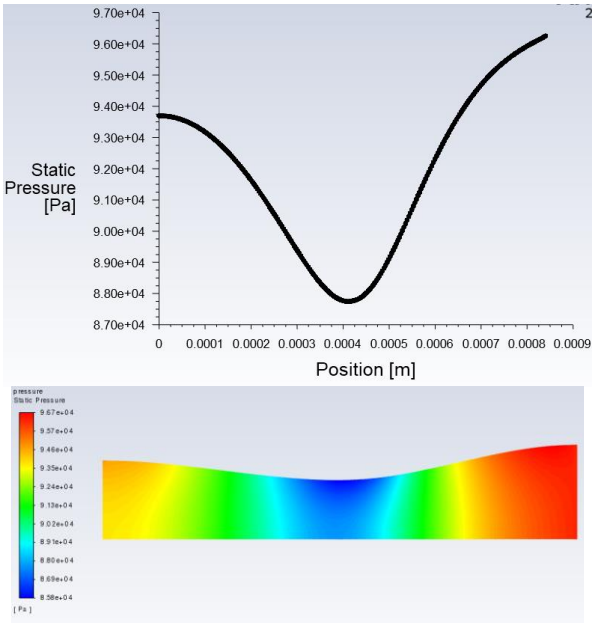

Figure 6. Static pressure contour for Pr = 0.95

In this first case, with Pr of 0.95, results follow expected trends. As velocity (shown as Mach number in Fig. 5) increases, pressure decreases proportionally. Additionally, velocity increases to a maximum of Mach 0.49 at the throat and decreases back down to Mach 0.25 at the nozzle's exit. As expected, this pressure ratio is too low to allow for sonic or supersonic flow.

Case II.

Mach number and static pressure for case II are shown above. A sharp decrease in velocity and increase in static pressure is seen at 0.6mm. This sudden change is caused by a normal shock, arising from a mismatch between back and exit pressure. While the flow reaches sonic speed at the throat and accelerates to Mach 1.59, the shock causes it to slow down to subsonic speeds, and the diffuser causes the flow to further slowdown to Mach 0.35.

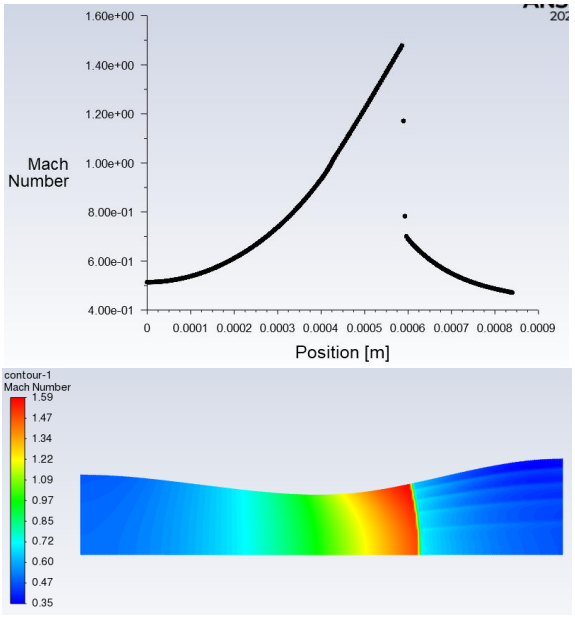

Figure 7. Mach number contour for Pr = 0.8

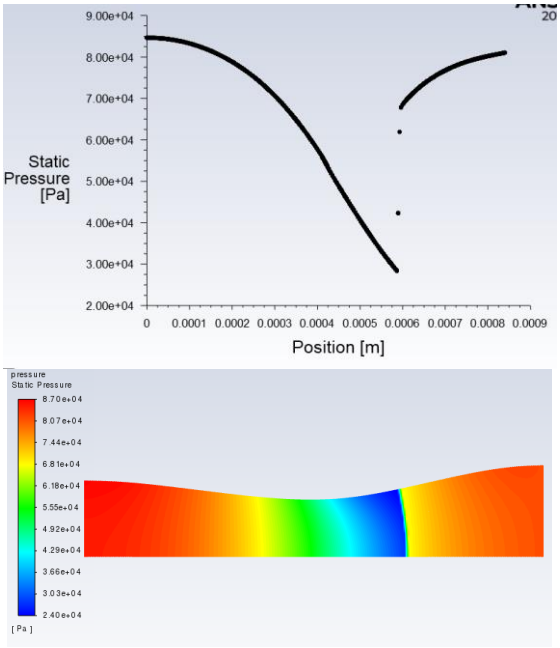

Figure 8. Static pressure contour for Pr = 0.8

Case III.

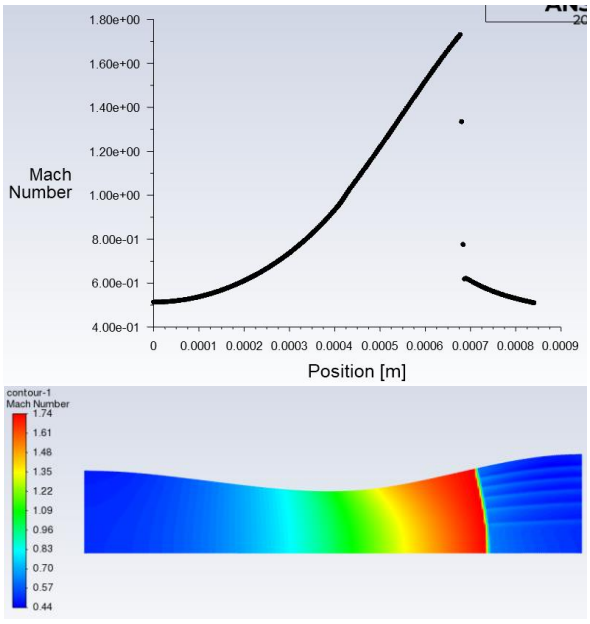

Figure 9. Mach number contour for Pr = 0.7

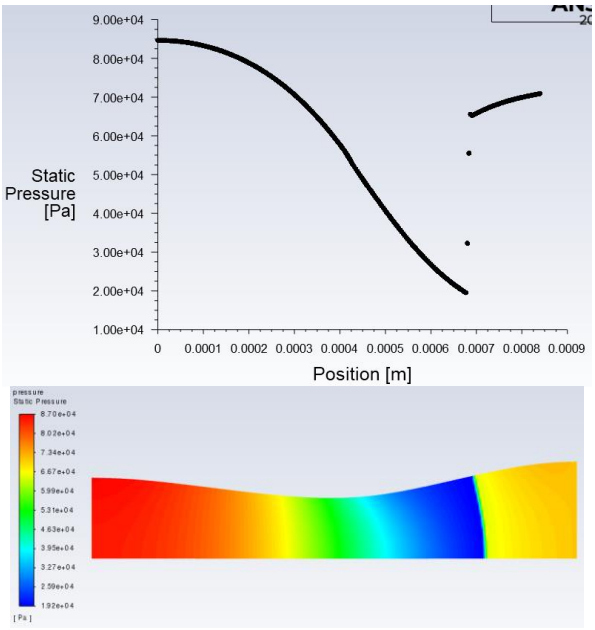

Figure 10. Static pressure contour for Pr = 0.7

Similar to case II, case III has a shock in the nozzle's diffuser, causing a sudden drop in velocity and rise in pressure. However, the shock is noticeably further away from the throat,

occurring at 0.7mm. As such, the flow's maximum velocity is Mach 1.74, when the static pressure is $1.92x10^4$.

Case IV.

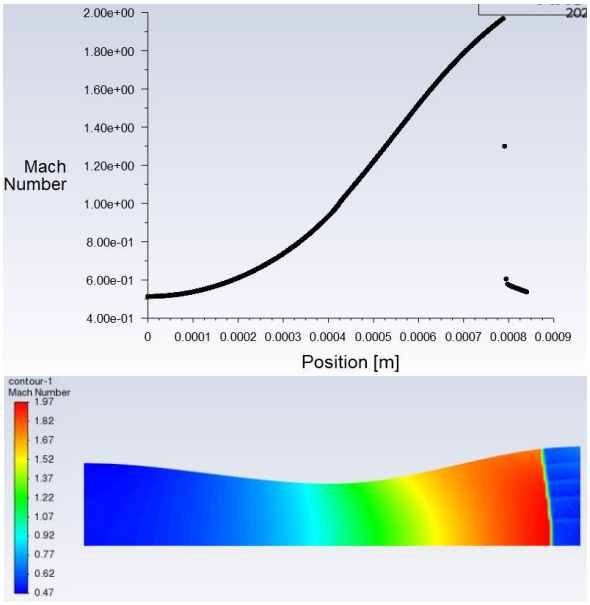

Figure 11. Mach number contour for Pr = 0.6

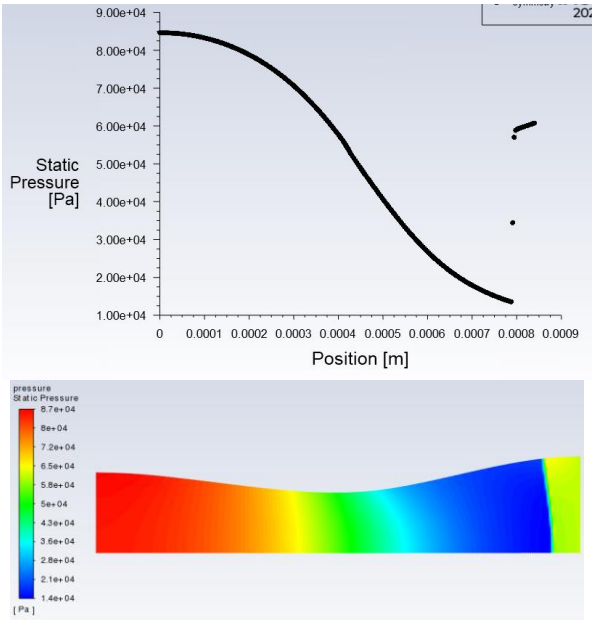

Figure 12. Static pressure contour for Pr = 0.6

Figures 11 and 12 show that the pressure ratio is almost optimal for this De-Laval nozzle with initial conditions stated in Table III. The shock has moved further towards the outlet, indicating that the appropriate back pressure to obtain a fully supersonic nozzle has almost been reached.

Case V.

Figures 13 and 14 show an almost fully supersonic nozzle, reaching a maximum velocity of Mach 2.05 and minimum static pressure of $1.19x10^4$ Pa at the outlet. However, there is a shock at the outlet. This was unexpected as the nozzle was expected to be fully supersonic with a pressure ratio as low as 0.5. As such one final case, with a pressure ratio of 0.4 was tested to investigate this result.

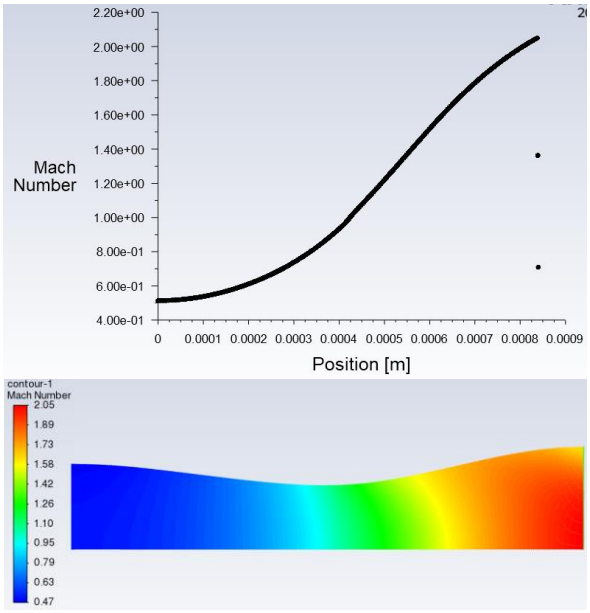

Figure 13. Mach number contour for Pr = 0.5

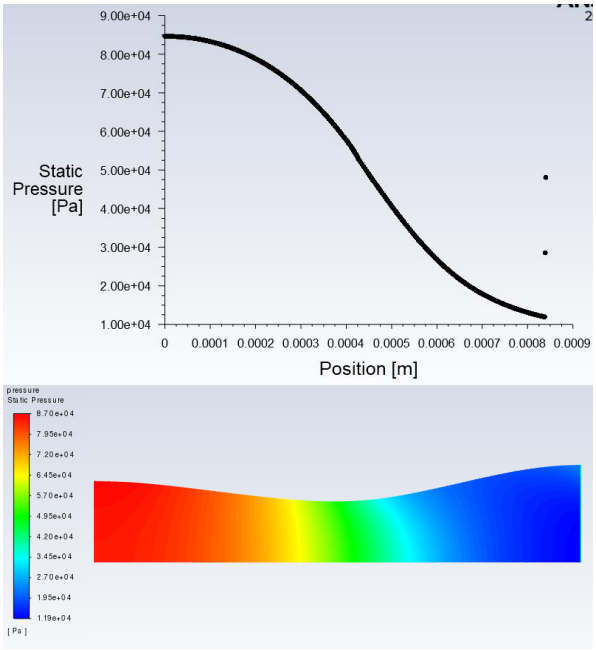

Figure 14. Static pressure contour for Pr = 0.5

Case VI.

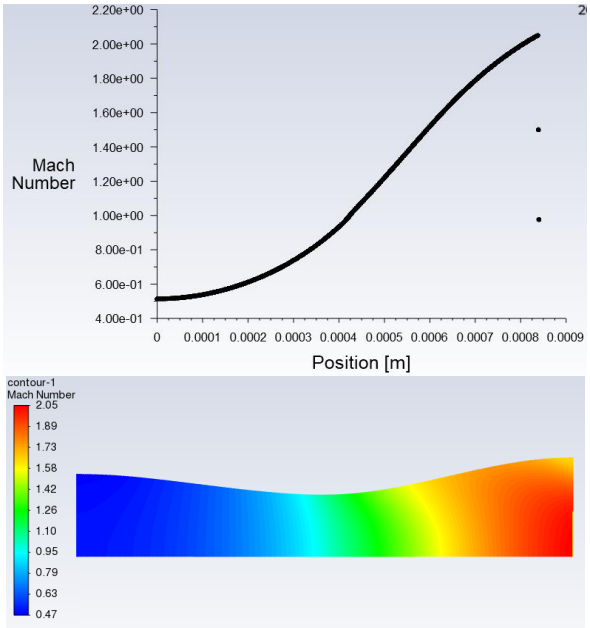

Figure 15. Mach number contour for Pr = 0.4

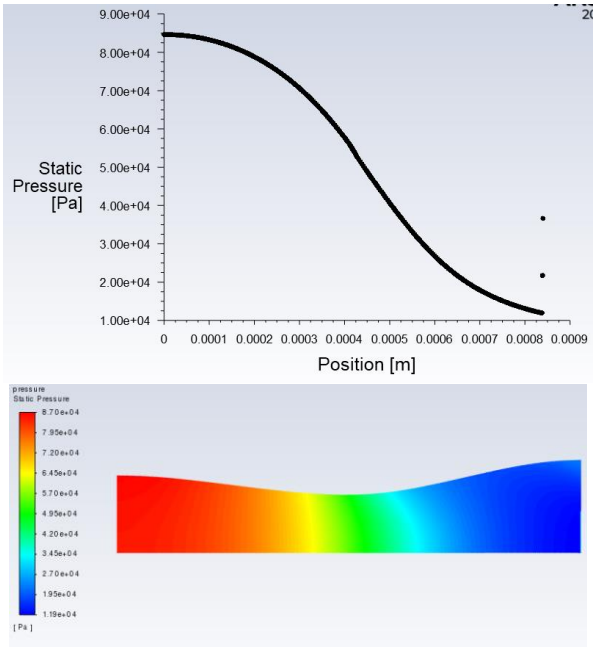

Figure 16. Static pressure contour for Pr = 0.4

While the nozzle seems to be fully supersonic with Pr = 0.4, a small low velocity and high-pressure region can be seen on the outlet's lower half. However, the velocity and pressure profiles for both cases V and VI are similar. This hints at an issue with either the mesh or the models used to solve these cases.

IV. Conclusion

While the initial aim of this report was to model ‘real’ viscous flow, other models were used, yet due to issues with the software and results (discussed in Appendix B), only inviscid flow was modeled. Nevertheless, the results calculated by ANSYS Fluent follow real-world trends, with the flow being unable to reach sonic speeds at high-pressure ratios, going supersonic, but slowing down due to normal shocks at intermediate pressure ratios, and finally being fully supersonic at low-pressure ratios. However, a shock occurred at the outlet for low-pressure ratios, yet, this is most likely due to the inviscid model used, as similar issues occurred in scholarly papers [8]. As such, it can be determined that the optimal pressure ratio for a supersonic nozzle lies between Pr=0.6 and Pr=0.5.

All in all, I learned a lot about using ANSYS software to create cases and solve them using numerical analysis methods focused on CFD. Through numerous YouTube tutorials, scratching my head to understand why a case was not converging (and doing the opposite), I was able to get a better grasp of a commercial CFD software. In the future, I hope to be able to model viscous flow and learn more about the numerous models available in the Fluent software.

References

[1] Goodman, N., Leege, B. J., and Johnson, P. E., "An improved de Laval nozzle experiment," *International Journal of Mechanical Engineering Education,* Aug. 2021.

[2] Ozman, A. H., and Abdelhameed, H. E., "CFD Analysis of De Laval Nozzle Geometry & Effect of Gas Pressure Variation at the Entrance," *Engineering, Technology and Applied Science Research,* Dec. 2018.

[3] Devenport, W. J., "Converging Diverging Nozzle," Available: https://www.engapplets.vt.edu/fluids/CDnozzle/cdinfo.html.

[4] "Supersonic nozzle simulation in Ansys Fluent - part 1," Chemical Propulsion Laboratory at the University of Brasilia, Available: https://youtu.be/yIrGUPm-1mM.

[5] "ANSYS FLUENT 12.0 User's Guide - First-Order Accuracy vs. Second-Order Accuracy," ANSYS, Inc, Jan. 2009. Available: https://wwwafs.portici.enea.it/project/neptunius/docs/fluent/html/ug/node779.htm

[6] Patankar, S. V. "Numerical Heat Transfer and Fluid Flow," Taylor & Francis, 1980. ISBN 978-0-89116-522-4.

[7] Cummings, M. "Applied Computational Aerodynamics: A Modern Engineering Approach," Cambridge Aerospace Series, 2015. ISBN: 9781107053748.

[8] Singh, K. P., Tripathi, A., "CFD ANALYSIS OF DE-LAVAL NOZZLE," *IJARIIE*, Vol. 3, 2017.

Appendix

Appendix A – Graph of residuals for each test case.

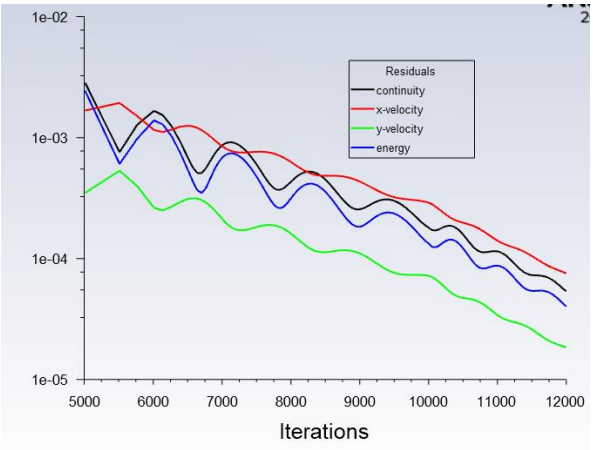

Figure A.1. Residuals for Pr=0.95

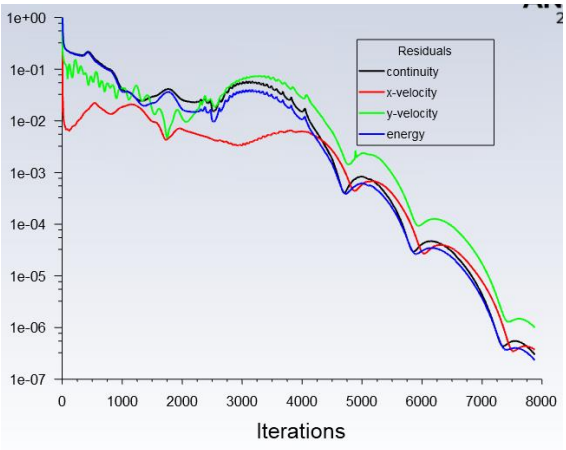

Figure A.2. Residuals for Pr=0.8

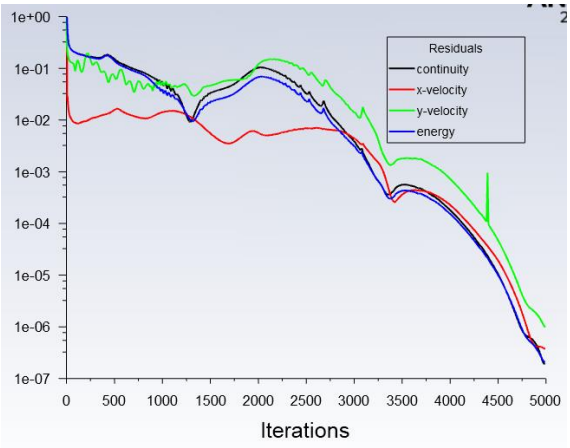

Figure A.3. Residuals for Pr=0.7

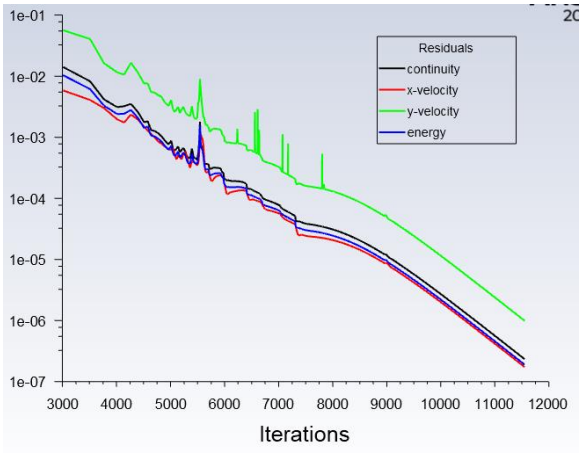

Figure A.4. Residuals for Pr=0.6

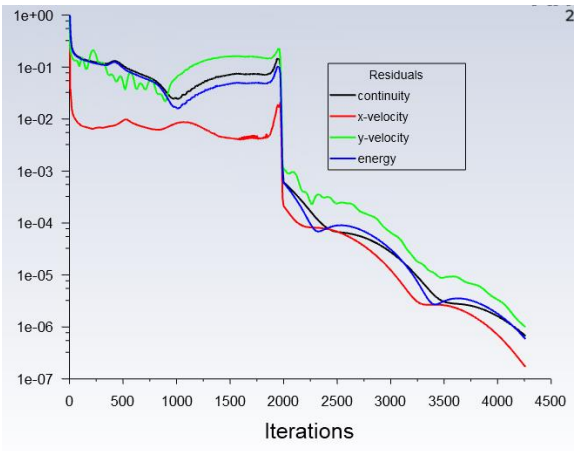

Figure A.4. Residuals for Pr=0.5

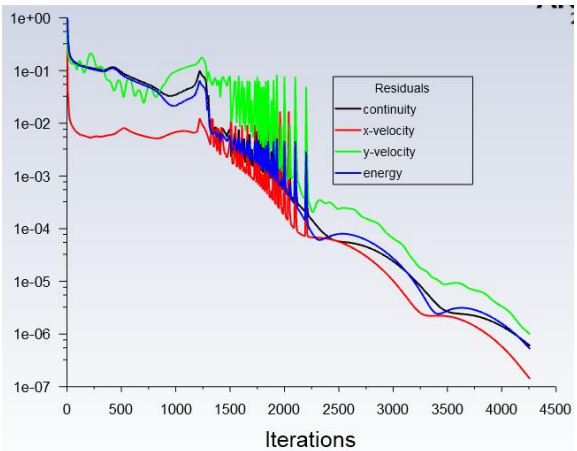

Figure A.4. Residuals for Pr=0.4

Appendix B

Throughout numerous days of working on the Georgia Tech VLab to use ANSYS fluent, I had to change my geometry, meshing, and operating conditions numerous times for Fluent to converge towards a steady state answer. After watching a video explaining how to do inviscid and viscous flow of a De-Laval nozzle, I decided to start by doing all cases using an inviscid model. Once all inviscid data had been collected, I imported the inviscid data and ran the case with viscous flow. Yet, once the case had converged, the Fluent app crashed numerous times without me screenshotting any data. After numerous restarts, I realized that it was possible to save cases and data, which helped ensure that all my work (mainly waiting for fluent) wouldn't disappear due to the unstable or low-performance VLab. However, this often made Fluent crash, and if it did not, the resulting data would not be accurate, as shown in Figure B.1, which was taken before Fluent shut down.

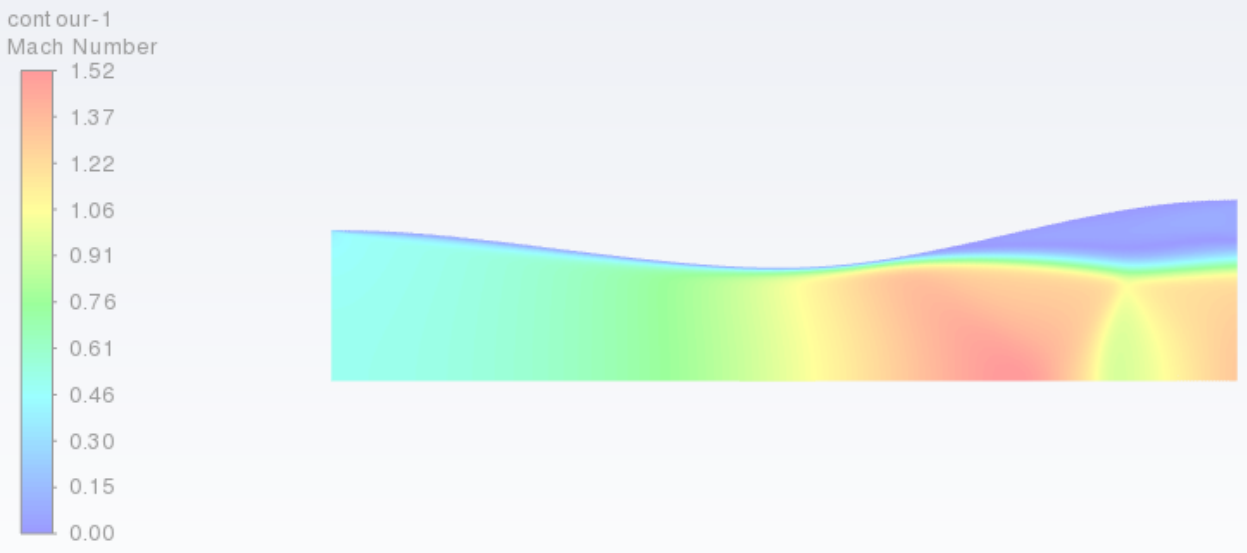

Figure B.1. Mach number contour for Pr=0.4

Figure B.1. was taken as the case was almost converged (I was not able to take a screenshot of the residuals as Fluent was stuck on this screen), with all residuals under 1e-6. The method was changed to second order upwind to ensure Fluent would be able to accurately solve the case. The first half of the nozzle seems to have accurate results, with a thin boundary layer at the wall, and the flow going supersonic at the throat. Yet rather than increasing after the throat, velocity behaves in unexpected ways, and the boundary layer grows massively, which incorrect.